




Intercalant-mediated Kitaev exchange in $\text{Ag}_3\text{LiIr}_2\text{O}_6$ Ravi Yadav,^{1,2} Sahinur Reja,^{3,4} Rajyavardhan Ray ,^{5,6} Jeroen van den Brink,^{5,7} Satoshi Nishimoto ,^{5,7} and Oleg V. Yazyev ^{1,2}¹*Institute of Physics, Ecole Polytechnique Fédérale de Lausanne (EPFL), CH-1015 Lausanne, Switzerland*²*National Centre for Computational Design and Discovery of Novel Materials MARVEL, Ecole Polytechnique Fédérale de Lausanne (EPFL), CH-1015 Lausanne, Switzerland*³*Department of Physics, School of Physical Sciences, Central University of Rajasthan, Bandarsindri, Kishangarh-305817, Rajasthan, India*⁴*Department of Physics, Jadavpur University, Kolkata 700032, India*⁵*Institute for Theoretical Solid State Physics, IFW Dresden, 01069 Dresden, Germany*⁶*Dresden Center for Computational Material Science (DCMS), TU Dresden, 01062 Dresden, Germany*⁷*Department of Physics, Technische Universität Dresden, 01062 Dresden, Germany*

(Received 11 November 2021; revised 24 April 2022; accepted 1 June 2022; published 11 July 2022)

The recently synthesized $\text{Ag}_3\text{LiIr}_2\text{O}_6$ has been proposed as a Kitaev magnet in proximity to the quantum spin liquid phase. We explore its microscopic Hamiltonian and magnetic ground state using many-body quantum chemistry methods and exact diagonalization techniques. Our calculations establish a dominant bond dependent ferromagnetic Kitaev exchange between Ir sites and find that the inclusion of Ag $4d$ orbitals in the configuration interaction calculations strikingly enhances the Kitaev exchange. Furthermore, using exact diagonalization of the nearest-neighbor fully anisotropic J - K - Γ Hamiltonian, we obtain the magnetic phase diagram as a function of further neighbor couplings. We find that the antiferromagnetic off-diagonal coupling stabilizes long range order, but the structure factor calculations suggest that the material is very close to the quantum spin liquid phase and the ordered state can easily collapse into a liquid by small perturbations such as structural distortion or bond disorder.

DOI: [10.1103/PhysRevResearch.4.033025](https://doi.org/10.1103/PhysRevResearch.4.033025)

Introduction. The search for quantum spin liquid (QSL) in honeycomb lattice systems has triggered intense research activity in the condensed matter community during the past decade [1–3]. QSL's are especially interesting for the field of quantum computing and information as they exhibit elementary excitations, which are a characteristic of the Majorana fermions. The Kitaev model is particularly interesting in this context as it is known to host QSL ground states [3–5]. The Kitaev Hamiltonian considers the diagonal part of anisotropic bond-dependent magnetic interactions between nearest neighbor (NN) spin states on honeycomb lattice [4]. However, in real-world materials, the Kitaev interaction (K) is often accompanied by the competing isotropic Heisenberg coupling (J) and off-diagonal anisotropic couplings (Γ). This generalized spin model (commonly referred as the J - K - Γ model) is known to have a more complex phase diagram as these additional parameters can change the ground state depending on their magnitude and signs.

Extensive investigations have been carried out on honeycomb lattice iridates with the general formula A_2IrO_3 ($A = \text{Na}, \text{Li}, \text{K}, \text{Cu}$) [3,6–13] and their derivatives [14,15] as well as α - RuCl_3 [1,16,17]. All of these systems have layered

crystal structures, in which each layer consists of transition metal (TM) forging edge-sharing octahedra with ligand and the TM ions form a honeycomb network. The magnitude of anisotropic as well as isotropic couplings is crucial for stabilizing spin liquid states in these materials. For the known honeycomb materials, the reported ratio $|K/J| \approx 4 - 8$ implies strong anisotropic magnetic interactions [10,14,15,17]. However, a conventional long range magnetic order is realized instead, due to small but significant NN Heisenberg coupling (J) as well as longer range Heisenberg exchange interactions. Additionally, the lower symmetry in these systems allows the existence of off-diagonal anisotropic couplings, which have been recently investigated for their effect on the magnetic ground states in honeycomb lattice systems [10,18,19].

Furthermore, the tunable nature of isotropic and anisotropic couplings with various factors such as structural modifications, inter or intra-layer electrostatics and strength of spin-orbit coupling (SOC) has motivated the search and investigation of materials realizing the Kitaev model with favorable ratios of the corresponding magnetic exchange parameters [20–23]. The recently reported $\text{Ag}_3\text{LiIr}_2\text{O}_6$ is being explored in this context [24–26].

In this Letter, we address the exchange interactions between two Ir sites in $\text{Ag}_3\text{LiIr}_2\text{O}_6$ using highly accurate many-body quantum chemistry calculations. Our results obtained at the configuration interaction level of theory show that the $4d$ orbitals corresponding to Ag enhance anisotropic interaction parameters (K and Γ) by directly participating in the superexchange process, and significantly increase the ratio

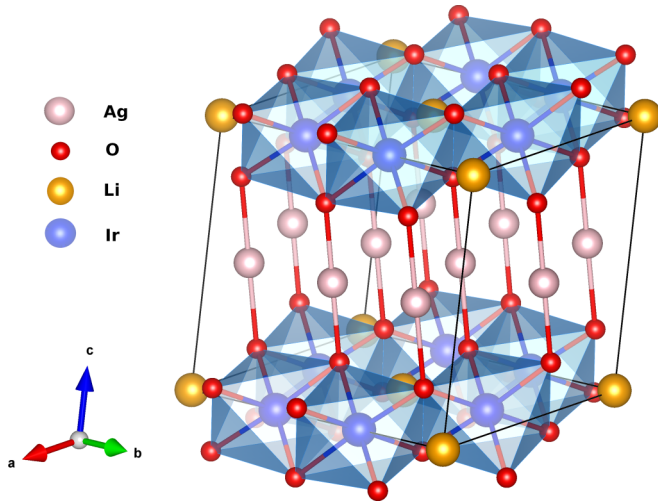


FIG. 1. Honeycomb network formed by edge sharing IrO_6 octahedra in $\text{Ag}_3\text{LiIr}_2\text{O}_6$. The Ag^+ ions are located in such a way that an interlayer connectivity is realized through linear O-Ag-O chains [23].

of anisotropic to isotropic couplings. Further, we obtained the magnetic phase diagram as a function of the second (J_2) and third neighbor (J_3) Heisenberg exchange parameters using exact diagonalization (ED) for the fully anisotropic Hamiltonian derived from quantum chemistry calculations. We find that this system would form a long-range magnetic order of zigzag antiferromagnetic (AFM) type, as the AFM Γ_{yz} couplings tends to counteract the FM Kitaev interactions and drive the system away from the QSL phase. However, the ED calculations reveal that the static structure factor for $\text{Ag}_3\text{LiIr}_2\text{O}_6$ is quite similar to that of Kitaev spin liquid phase suggesting a close proximity to the spin liquid phase.

Atomic and electronic structure. The structural details of $\text{Ag}_3\text{LiIr}_2\text{O}_6$ were reported by Bahrami *et al.* [23] and Bette *et al.* [27] independently. It is synthesized by chemical substitution of Li^+ ions located between the honeycomb planes in $\alpha\text{-Li}_2\text{IrO}_3$ by Ag^+ ions [23,27]. $\text{Ag}_3\text{LiIr}_2\text{O}_6$ displays a layered structure where edge-shared IrO_6 octahedra constitute the planar honeycomb-like network as shown in Fig. 1. A Li^+ ion occupies the center of each hexagon, as in the parent compound $\alpha\text{-Li}_2\text{IrO}_3$. The major structural difference comes from the fact that the interlayer Ag^+ ions sandwiched between two honeycomb planes occupy slightly different positions than the Li^+ ions in the parent compound, giving rise to linear O-Ag-O bonds. This system is structurally similar to another reported derivative of $\alpha\text{-Li}_2\text{IrO}_3$, namely $\text{H}_3\text{LiIr}_2\text{O}_6$, where interlayer Li^+ ions are replaced by H^+ ions [21]. However, $\text{Ag}_3\text{LiIr}_2\text{O}_6$ is unique in the sense that $4d$ orbitals of the Ag^+ ions can hybridize with the O $2p$ orbitals and can also participate in superexchange between NN Ir $5d$ shells.

The Ir $5d$ levels are split into e_g and t_{2g} states due to the octahedral ligand field. The t_{2g} states lie at a significantly lower energy [28], making Ir t_{2g}^5 as the leading ground-state configuration and yielding an effective picture of one hole in the t_{2g} sector. In the presence of strong spin-orbit coupling, this can be mapped onto a set of fully occupied $j_{\text{eff}} = 3/2$ and half-filled $j_{\text{eff}} = 1/2$ states [29–31]. Deviations from a perfect

TABLE I. NN magnetic couplings (in meV) for the two different bonds B1 and B2 in $\text{Ag}_3\text{LiIr}_2\text{O}_6$ using the structural data from Ref. [23]; results of spin-orbit MRCI calculations are shown.

Bond	$\angle\text{Ir-O-Ir}$	K	J	Γ_{xy}	$\Gamma_{yz} = -\Gamma_{zx}$
B2 (3.06Å)	96.8°	-11.2	-0.3	-1.3	4.9
B1 (3.05Å)	92.8°	-10.1	-0.9	-1.0	2.8

cubic environment may lead to some degree of admixture of these $j_{\text{eff}} = 1/2$ and $j_{\text{eff}} = 3/2$ components.

Similar to the parent compound $\alpha\text{-Li}_2\text{IrO}_3$, two structurally different types of Ir-Ir links are present in this system [21]. For each of these links, the unit of two NN octahedra displays C_{2h} point-group symmetry, which then implies a generalized bilinear Hamiltonian of the following form for a pair of pseudospins i and j

$$\mathcal{H}_{ij} = J \tilde{S}_i \cdot \tilde{S}_j + K \tilde{S}_i^z \tilde{S}_j^z + \sum_{\alpha \neq \beta} \Gamma_{\alpha\beta} (\tilde{S}_i^\alpha \tilde{S}_j^\beta + \tilde{S}_i^\beta \tilde{S}_j^\alpha), \quad (1)$$

where the $\Gamma_{\alpha\beta}$ coefficients refer to the off-diagonal components of the symmetric anisotropic exchange matrix, with $\alpha, \beta \in \{x, y, z\}$. An antisymmetric Dzyaloshinskii-Moriya (DM) coupling is not allowed, given the inversion center for each block of two NN octahedra. A local Kitaev reference frame is used here, such that for each Ir-Ir link the z axis is perpendicular to the Ir_2O_2 plaquette.

Calculation of magnetic interactions. The magnetic exchange couplings between two NN Ir sites were obtained from quantum chemistry calculations on embedded clusters with two edge-sharing octahedra as the central region. The four adjacent IrO_6 octahedra were also included in the calculations to account for the finite charge distribution in the immediate neighborhood, while arrays of point charges fitted to reproduce the ionic Madelung potential in the cluster region were used to model the solid-state environment. As a first step, we obtained multiconfiguration wavefunctions at the complete-active-space self-consistent-field (CASSCF) level of theory, where optimized wavefunctions were obtained for an average of the lowest nine singlet and nine triplet states. In the second step, the CASSCF wave functions are used in the multireference configuration-interaction (MRCI) calculations, allowing single and double excitations from the Ir $5d$ (t_{2g}) and the bridging-ligand $2p$ valence shells.

The spin-orbit computations were performed in terms of the low-lying nine singlet and nine triplet states. The lowest four *ab initio* spin-orbit eigenstates were mapped onto the eigenvectors of the effective spin Hamiltonian (1). The other 32 spin-orbit states in this manifold involve $j_{\text{eff}} \approx 3/2$ to $j_{\text{eff}} \approx 1/2$ excitations and lie at a significantly higher energy [14,28,32]. The mapping of the *ab initio* data onto the effective spin Hamiltonian is carried out following the procedure described in Refs. [17,33,34]. All quantum chemistry computations were performed using the quantum chemistry package MOLPRO [35].

Effective magnetic exchange interactions obtained using the procedure mentioned above are listed for the experimental structural data reported in Ref. [23] in Table I. Not all six links connecting Ir-Ir sites are equal, but vary slightly in their length

($\delta d = 0.12 \text{ \AA}$). For both types of Ir-Ir links, the Kitaev coupling K is ferromagnetic, with $K = -11.2 \text{ meV}$ for the longer bond. The $|K/J|$ ratio is high, which in principle indicates that the system is close to the pure Kitaev limit. However, we also find that the off-diagonal exchange anisotropy Γ_{yz} (allowed due to lower symmetry) has a considerable magnitude. It is AFM in nature and can counteract the frustration brought in by FM Kitaev couplings.

Phase diagram and longer-range interactions. From the NN magnetic interactions in Table I, $\text{Ag}_3\text{LiIr}_2\text{O}_6$ appears to be close to realizing the Kitaev model, indicated by the larger $|K/J|$ ratio compared to other $A_2\text{IrO}_3$ ($A = \text{Li, Na}$) iridates and their derivatives considered so far. It is known that in the $A_2\text{IrO}_3$ systems, the experimentally observed zigzag ordered state at low temperature is stabilized not only by the residual NN isotropic couplings, but also by the longer-range magnetic interactions that are present, even if the latter can be weak [17,22,32]. In order to assess the magnetic ground state of $\text{Ag}_3\text{LiIr}_2\text{O}_6$, we obtained the phase diagram using the NN quantum chemistry coupling parameters as a function of second-neighbor (J_2) and third-neighbor (J_3) isotropic Heisenberg parameters (see Fig. S1 in Ref. [36]). These calculations were performed as ED for a 24-site cluster with periodic boundary conditions as employed in earlier studies [3,14,32]. The phase boundaries were determined by the maximum positions in the second derivative of the ground-state energy. For a given set of J_2 and J_3 parameters, the dominant order was determined according to the wave number $\mathbf{Q} = \mathbf{Q}_{\max}$ providing a maximum value of the static structure factor $S(\mathbf{Q})$; the QSL state is characterized by the structureless $S(\mathbf{Q})$. Please see Ref. [36] for the detailed analysis. The phase diagram is quite distinct when compared to other known iridate counterparts [14,32,37], as the QSL phase is missing from the diagram. When comparing the magnetic couplings with the parameters reported for honeycomb systems [14,17,38–40], it becomes evident that there are two major differences: (i) the upturn in the $|K/J|$ ratio and (ii) an appreciable increase of the Γ_{yz} AFM coupling. The fact that higher $|K/J|$ ratios favour the QSL phase in the phase diagram suggests that an AFM Γ_{yz} is destabilizing the QSL region.

To test this hypothesis, we also mapped out the phase diagram in the Γ_{xy} - Γ_{yz} plane keeping other NN QC parameters and for $J_2 = J_3 = 0$ (assuming smaller long range interactions). The resulting phase diagram shown in Fig. 2 contains QSL phase for small value of Γ_{yz} , whereas $\text{Ag}_3\text{LiIr}_2\text{O}_6$ is represented by filled square in the zigzag phase. This clearly shows that the QSL region disappears as a result of AFM Γ_{yz} in $\text{Ag}_3\text{LiIr}_2\text{O}_6$. Experimental investigations also support the absence of QSL states in this material [23–25]. Furthermore, it is interesting to note that unlike other Kitaev materials the zigzag state can be stabilized by the Γ terms alone without considering longer-range interaction J_2, J_3 . However, we find that this zigzag phase is friable. In Fig. 3(b,c), the static structure factor for $\text{Ag}_3\text{LiIr}_2\text{O}_6$ is compared to that for Na_2IrO_3 , which is a typical example of zigzag state stabilized by finite J_2, J_3 . In $\text{Ag}_3\text{LiIr}_2\text{O}_6$, the weight spreads over a wide range of the hexagonal Brillouin zone, although the zigzag oscillations are dominant. This may suggest that the zigzag state of $\text{Ag}_3\text{LiIr}_2\text{O}_6$ is very close to QSL. In order to measure how close, we compare static structure factors of $\text{Ag}_3\text{LiIr}_2\text{O}_6$ to

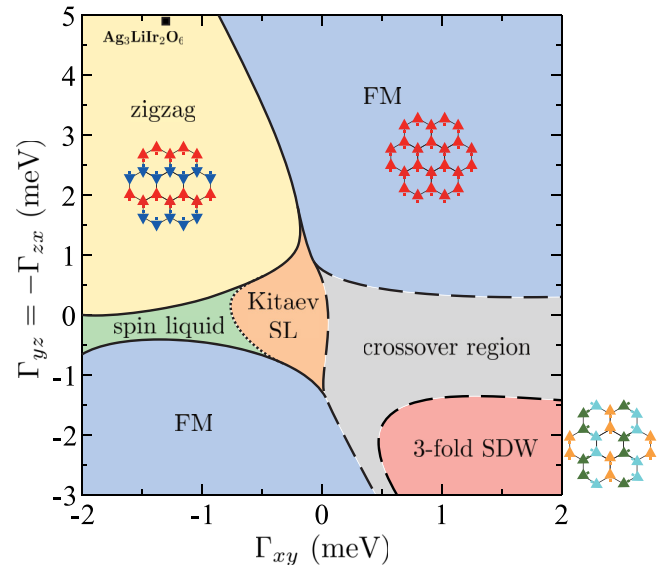


FIG. 2. Magnetic phase diagram in the $\Gamma_{xy} - \Gamma_{yz}$ plane for $J = -0.3 \text{ meV}$, $K = -11.2 \text{ meV}$, $J_2 = J_3 = 0 \text{ meV}$. Possible magnetic phases are shown along with schematic drawings of spin configurations.

that of the Kitaev-Heisenberg (KH) model. The static structure factors for the zigzag state of the KH model in the vicinity of the Kitaev SL phase are plotted in Fig. 3(d)–3(f). The

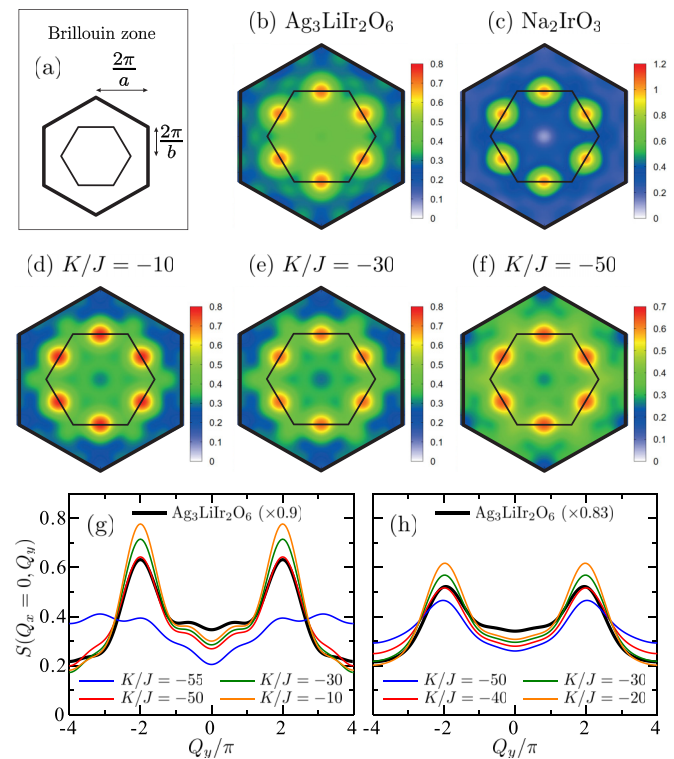


FIG. 3. (a) Brillouin zone, smaller hexagon being the first BZ; Structure factor plots for (b) $\text{Ag}_3\text{LiIr}_2\text{O}_6$, (c) Na_2IrO_3 [32], and (d)–(f) the Kitaev-Heisenberg model with parameters (in meV) as indicated; (g), (h) Static structure factor $S(Q_x = 0, Q_y)$ for (b), (d)–(f).

TABLE II. NN magnetic couplings obtained for the case where Ag^+ ions are represented as point charges. The values (in meV) correspond to spin-orbit MRCI results for the two bonds B1 and B2 in $\text{Ag}_3\text{LiIr}_2\text{O}_6$ using the structural data from Ref. [23].

Bond	$\angle\text{Ir-O-Ir}$	K	J	Γ_{xy}	$\Gamma_{yz} = -\Gamma_{zx}$
B2 (3.06Å)	96.8°	-5.1	0.9	-0.5	1.3
B1 (3.05Å)	92.8°	-4.6	0.8	-0.4	1.0

structure factor for $\text{Ag}_3\text{LiIr}_2\text{O}_6$ seems to be more similar to that for $|K/J| = 50$ than for $|K/J| = 10$ and $|K/J| = 30$. To be more precise, the shape of $S(Q_x = 0, Q_y)$ is compared in Fig. 3(g). We thus find that $\text{Ag}_3\text{LiIr}_2\text{O}_6$ compares well with $|K/J|$ ratios between 50 and 30 in the KH model. Also, interestingly, the expectation values of the hexagonal plaquette operator, indicating the closeness to Kitaev limit, are $\langle O_{\text{hp}} \rangle = 0.2801$ for $\text{Ag}_3\text{LiIr}_2\text{O}_6$ and $\langle O_{\text{hp}} \rangle = 0.2115$ for $|K/J| = 50$ (Ref. [36]). Since the critical point from zigzag to QSL is $|K/J| = 50.3$, $\text{Ag}_3\text{LiIr}_2\text{O}_6$ would be really proximal to QSL. Note that the same 24-site symmetric periodic cluster is used in all the above comparisons since this mapping is performed by using one-to-one correspondence between the two models. As shown in Fig. 3(h), a similar mapping using 24-site symmetric open cluster, which has much smaller finite-size effects on the stability of magnetic order than the periodic one, gives an effective ratio $|K/J| \sim 40$ for $\text{Ag}_3\text{LiIr}_2\text{O}_6$ against the zigzag-QSL critical point $|K/J| = 56.3$. Further analyses using various cluster sizes are demonstrated in Ref. [36] and all configurations support the proximity of $\text{Ag}_3\text{LiIr}_2\text{O}_6$ to the QSL phase. Thus, the zigzag state in $\text{Ag}_3\text{LiIr}_2\text{O}_6$ could be easily collapsed by small perturbations such as structural distortion, bond disorder, etc. This is consistent with the recent experimental observations.

The role of Ag 4d orbitals. It has been observed in a previous study that Ag 4d orbitals influence NN O 2p orbitals and could be vital for tuning exchange interactions in $\text{Ag}_3\text{LiIr}_2\text{O}_6$ [23]. In order to attain a comprehensive understanding of the role played by Ag^+ ions, we perform three different sets of quantum chemistry calculation. First, we treat the intercalant Ag^+ ions as point charges, such that these ions are not involved in the orbital optimization directly and their role is limited to providing electrostatic potential for the orbitals participating in the superexchange process. The magnetic couplings derived in this case are shown in Table II. In the second step, we include the Ag^+ ions in our calculations, allowing them to contribute to the wave function optimization at the CASSCF level of theory. However, in this step, the Ag^+ 4d orbitals are not included in the MRCI calculation, which implies that superexchange through the Ag^+ 4d orbitals is not allowed. The Kitaev coupling in this case is slightly increased to a magnitude of -5.7 meV from -5.1 meV obtained in step 1 (Table II). An interesting observation on the quantum-chemistry computational side is the significant enhancement of the Kitaev interactions as a result of including 4d orbitals of Ag^+ ions in the MRCI calculations in the third step, thus allowing superexchange through them along with the bridging O 2p orbitals (results are listed see Table I).

Another noteworthy observation is that magnetic couplings (in Table II) are weaker when compared to other known honeycomb iridates. This fact can be attributed to (i) Ir-O-Ir angles and (ii) the precise location of the inter-layer ionic species. The Ir-O-Ir angles in most honeycomb compounds become significantly larger due to trigonal compression of the oxygen cages. The smaller Ir-O-Ir bond angles imply a suppressed K , given the earlier estimates of K for angles in the range of 90° - 100° [17,32,37,39]. Additionally, the position of the inter-layer species directly above the bridging oxygen atoms have a direct influence on the exchange interactions, as also seen in iso-structural $\text{H}_3\text{LiIr}_2\text{O}_6$ [14,15,38]. The location of the inter-layer ionic species in Na_2IrO_3 and $\alpha\text{-Li}_2\text{IrO}_3$ is such that each O has six equidistant Na or Li NN, while the Ag-containing material has only one NN for each O [23,27]. In a purely ionic picture, the positive Ag^+ ion next to a given ligand generates an axial Coulomb potential that in principle affects the shape of the O 2p orbitals, thus influencing the in-plane Ir-Ir superexchange. This scenario was tested for the isostructural $\text{H}_3\text{LiIr}_2\text{O}_6$ using quantum chemistry as well as density functional calculations in earlier studies [14,38]. In other words, the strong reduction of the in-plane effective couplings in Table II compared to $\alpha\text{-Li}_2\text{IrO}_3$ and Na_2IrO_3 is also related to the negative effect of the Ag^+ cation Coulomb potential on the Ir-O-Ir superexchange. But, the direct involvement of the 4d orbitals of Ag^+ ion increases the Kitaev coupling in $\text{Ag}_3\text{LiIr}_2\text{O}_6$, which shows up in Table I.

Conclusions. In summary, using many-body quantum chemistry calculations, we find a large value for the $|K/J|$ ratio in $\text{Ag}_3\text{LiIr}_2\text{O}_6$, resulting from the involvement of 4d orbitals belonging to the interlayer Ag^+ cation in the superexchange process between two magnetically active Ir sites. Furthermore, using ED calculations for the derived magnetic couplings, we produced the magnetic phase diagram as a function of next neighbor coupling which suggests formation of long-range magnetic order as a result of the sizable AFM Γ_{yz} coupling. These results demonstrate that the strategy of replacing interlayer cations in $\alpha\text{-Li}_2\text{IrO}_3$ with Ag^+ ion acted in favor of enhancing the anisotropic exchange interactions; however, the off-diagonal anisotropic couplings are also lifted and counteract the frustration generated by Kitaev couplings. The ED calculations also reveal the proximity of the ground state to a QSL state, and the easily collapsible nature of ground state then necessitates a further tuning of the off-diagonal couplings. Such a fine tuning can be achieved as a result of small structural modifications, for example, by pressure or strain, which can steer this promising material towards realizing the QSL ground state.

Acknowledgements. R.Y. and O.V.Y. acknowledge the Swiss National Science Foundation (SNSF) Sinergia Network NanoSkyrmionics (Grant No. CRSII5-171003) and NCCR MARVEL for their financial support. R.R. thanks Manuel Richter for helpful discussions. S.R. acknowledge the financial support of DST-SERB (SRG/2020/001203) and UGC Grant F.30-528/2020(BSR). R.R. and S.N. acknowledge financial support from DFG through SFB 1143 Project No. A05. S.R. and S.N. acknowledge IFW/ITF computer cluster and thank Ulrike Nitzche for technical assistance.

- [1] A. Banerjee, C. A. Bridges, J.-Q. Yan, A. A. Aczel, L. Li, M. B. Stone, G. E. Granroth, M. D. Lumsden, Y. Yiu, J. Knolle, S. Bhattacharjee, D. L. Kovrizhin, R. Moessner, D. A. Tennant, D. G. Mandrus, and S. E. Nagler, Proximate Kitaev quantum spin liquid behaviour in a honeycomb magnet, *Nat. Mater.* **15**, 733 (2016).
- [2] J. Kim, M. Daghofer, A. H. Said, T. Gog, J. van den Brink, G. Khaliullin, and B. J. Kim, Excitonic quasiparticles in a spin-orbit Mott insulator, *Nat. Commun.* **5**, 4453 (2014).
- [3] J. Chaloupka, G. Jackeli, and G. Khaliullin, Kitaev-Heisenberg Model on a Honeycomb Lattice: Possible Exotic Phases in Iridium Oxides A_2IrO_3 , *Phys. Rev. Lett.* **105**, 027204 (2010).
- [4] A. Kitaev, Anyons in an exactly solved model and beyond, *Ann. Phys.* **321**, 2 (2006).
- [5] J. Chaloupka, G. Jackeli, and G. Khaliullin, Zigzag Magnetic order in the Iridium Oxide Na_2IrO_3 , *Phys. Rev. Lett.* **110**, 097204 (2013).
- [6] S. K. Choi, R. Coldea, A. N. Kolmogorov, T. Lancaster, I. I. Mazin, S. J. Blundell, P. G. Radaelli, Yogesh Singh, P. Gegenwart, K. R. Choi, S.-W. Cheong, P. J. Baker, C. Stock, and J. Taylor, Spin Waves and Revised Crystal Structure of Honeycomb Iridate Na_2IrO_3 , *Phys. Rev. Lett.* **108**, 127204 (2012).
- [7] S. H. Chun, J.-W. Kim, J. Kim, H. Zheng, C. C. Stoumpos, C. D. Malliakas, J. F. Mitchell, K. Mehlawat, Y. Singh, Y. Choi, T. Gog, A. Al-Zein, M. M. Sala, M. Krisch, J. Chaloupka, G. Jackeli, G. Khaliullin, and B. J. Kim, Direct evidence for dominant bond-directional interactions in a honeycomb lattice iridate Na_2IrO_3 , *Nat. Phys.* **11**, 462 (2015).
- [8] Y. Singh, S. Manni, J. Reuther, T. Berlijn, R. Thomale, W. Ku, S. Trebst, and P. Gegenwart, Relevance of the Heisenberg-Kitaev Model for the Honeycomb Lattice Iridates A_2IrO_3 , *Phys. Rev. Lett.* **108**, 127203 (2012).
- [9] I. I. Mazin, S. Manni, K. Foyevtsova, Harald O. Jeschke, P. Gegenwart, and Roser Valentí, Origin of the insulating state in honeycomb iridates and rhodates, *Phys. Rev. B* **88**, 035115 (2013).
- [10] R. Yadav, S. Nishimoto, M. Richter, J. van den Brink, and R. Ray, Large off-diagonal exchange couplings and spin liquid states in C_3 -symmetric iridates, *Phys. Rev. B* **100**, 144422 (2019).
- [11] R. D. Johnson, I. Broeders, K. Mehlawat, Y. Li, Y. Singh, R. Valentí, and R. Coldea, Chemical tuning between triangular and honeycomb structures in a $5d$ spin-orbit Mott insulator, *Phys. Rev. B* **100**, 214113 (2019).
- [12] K. Mehlawat and Y. Singh, Quantum spin liquid in a depleted triangular lattice iridate $K_xIr_yO_2$, arXiv preprint [arXiv:1908.08475](https://arxiv.org/abs/1908.08475) (2019).
- [13] M. Abramchuk, C. O. Keskinbora, J. W. Krizan, K. R. Metz, D. C. Bell, and F. Tafti, Cu_2IrO_3 : a new magnetically frustrated honeycomb iridate, *J. Am. Chem. Soc.* **139**, 15371 (2017).
- [14] R. Yadav, R. Ray, M. S. Eldeeb, S. Nishimoto, L. Hozoi, and J. van den Brink, Strong Effect of Hydrogen Order on Magnetic Kitaev Interactions in $H_3LiIr_2O_6$, *Phys. Rev. Lett.* **121**, 197203 (2018).
- [15] R. Yadav, M. S. Eldeeb, R. Ray, S. Aswartham, M. I. Sturza, S. Nishimoto, J. van den Brink, and L. Hozoi, Engineering Kitaev exchange in stacked iridate layers: impact of inter-layer species on in-plane magnetism, *Chem. Sci.* **10**, 1866 (2019).
- [16] K. W. Plumb, J. P. Clancy, L. J. Sandilands, V. Vijay Shankar, Y. F. Hu, K. S. Burch, Hae-Young Kee, and Young-June Kim, α - $RuCl_3$: A spin-orbit assisted Mott insulator on a honeycomb lattice, *Phys. Rev. B* **90**, 041112(R) (2014).
- [17] R. Yadav, N. A. Bogdanov, V. M. Katukuri, S. Nishimoto, J. van den Brink, and L. Hozoi, Kitaev exchange and field-induced quantum spin-liquid states in honeycomb α - $RuCl_3$, *Sci. Rep.* **6**, 37925 (2016).
- [18] I. Rousochatzakis and N. B. Perkins, Classical Spin Liquid Instability Driven By Off-Diagonal Exchange in Strong Spin-Orbit Magnets, *Phys. Rev. Lett.* **118**, 147204 (2017).
- [19] P. Lampen-Kelley, S. Rachel, J. Reuther, J.-Q. Yan, A. Banerjee, C. A. Bridges, H. B. Cao, S. E. Nagler, and D. Mandrus, Anisotropic susceptibilities in the honeycomb kitaev system α - $rucl_3$, *Phys. Rev. B* **98**, 100403(R) (2018).
- [20] G. Bastien, G. Garbarino, R. Yadav, F. J. Martinez-Casado, R. Beltrán Rodríguez, Q. Stahl, M. Kusch, S. P. Limandri, R. Ray, P. Lampen-Kelley, D. G. Mandrus, S. E. Nagler, M. Roslova, A. Isaeva, T. Doert, L. Hozoi, A. U. B. Wolter, B. Büchner, J. Geck, and J. van den Brink, Pressure-induced dimerization and valence bond crystal formation in the Kitaev-Heisenberg magnet α - $RuCl_3$, *Phys. Rev. B* **97**, 241108(R) (2018).
- [21] K. Kitagawa, T. Takayama, Y. Matsumoto, A. Kato, R. Takano, Y. Kishimoto, S. Bette, R. Dinnebier, G. Jackeli, and H. Takagi, A spin-orbital-entangled quantum liquid on a honeycomb lattice, *Nature (London)* **554**, 341 (2018).
- [22] M. Majumder, R. S. Manna, G. Simutis, J. C. Orain, T. Dey, F. Freund, A. Jesche, R. Khasanov, P. K. Biswas, E. Bykova, N. Dubrovinskaia, L. S. Dubrovinsky, R. Yadav, L. Hozoi, S. Nishimoto, A. A. Tsirlin, and P. Gegenwart, Breakdown of Magnetic Order in the Pressurized Kitaev Iridate β - Li_2IrO_3 , *Phys. Rev. Lett.* **120**, 237202 (2018).
- [23] F. Bahrami, W. L. D. Hauret, O. I. Lebedev, R. Movshovich, H. Y. Yang, D. Broido, X. Rocquefelte, and F. Tafti, Thermodynamic Evidence of Proximity to a Kitaev Spin Liquid in $Ag_3LiIr_2O_6$, *Phys. Rev. Lett.* **123**, 237203 (2019).
- [24] F. Bahrami, E. M. Kenney, C. Wang, A. Berlie, O. I. Lebedev, M. J. Graf, and F. Tafti, Effect of structural disorder on the Kitaev magnet $Ag_3LiIr_2O_6$, *Phys. Rev. B* **103**, 094427 (2021).
- [25] J. Wang, W. Yuan, T. Imai, P. M. Singer, F. Bahrami, and F. Tafti, NMR investigation on the honeycomb iridate $Ag_3LiIr_2O_6$, *Phys. Rev. B* **103**, 214405 (2021).
- [26] A. Chakraborty, V. Kumar, S. Bachhar, N. Büttgen, K. Yokoyama, P. K. Biswas, V. Siruguri, Sumiran Pujari, I. Dasgupta, and A. V. Mahajan, Unusual spin dynamics in the low-temperature magnetically ordered state of $Ag_3LiIr_2O_6$, *Phys. Rev. B* **104**, 115106 (2021).
- [27] S. Bette, T. Takayama, V. Duppel, A. Poulain, H. Takagi, and R. E. Dinnebier, Crystal structure and stacking faults in the layered honeycomb, delafossite-type materials $Ag_3LiIr_2O_6$ and $Ag_3LiRu_2O_6$, *Dalton Trans.* **48**, 9250 (2019).
- [28] H. Gretarsson, J. P. Clancy, X. Liu, J. P. Hill, Emil Bozin, Yogesh Singh, S. Manni, P. Gegenwart, Jungho Kim, A. H. Said, D. Casa, T. Gog, M. H. Upton, Heung-Sik Kim, J. Yu, Vamshi M. Katukuri, L. Hozoi, Jeroen van den Brink, and Young-June Kim, Crystal-Field Splitting and Correlation Effect on the Electronic Structure of A_2IrO_3 , *Phys. Rev. Lett.* **110**, 076402 (2013).
- [29] G. Jackeli and G. Khaliullin, Mott Insulators in the Strong Spin-Orbit Coupling Limit: From Heisenberg to a Quantum Compass and Kitaev Models, *Phys. Rev. Lett.* **102**, 017205 (2009).

- [30] A. Abragam and B. Bleaney, *Electron Paramagnetic Resonance of Transition Ions* (Clarendon Press, Oxford, 1970).
- [31] B. J. Kim, Hosub Jin, S. J. Moon, J.-Y. Kim, B.-G. Park, C. S. Leem, Jaejun Yu, T. W. Noh, C. Kim, S.-J. Oh, J.-H. Park, V. Durairaj, G. Cao, and E. Rotenberg, Novel $J_{\text{eff}} = 1/2$ Mott state Induced by Relativistic Spin-Orbit Coupling in Sr_2IrO_4 , *Phys. Rev. Lett.* **101**, 076402 (2008).
- [32] V. M. Katukuri, S. Nishimoto, V. Yushankhai, A. Stoyanova, H. Kandpal, S. Choi, R. Coldea, I. Rousochatzakis, L. Hozoi, and J. van den Brink, Kitaev interactions between $j = 1/2$ moments in honeycomb Na_2IrO_3 are large and ferromagnetic: insights from ab initio quantum chemistry calculations, *New J. Phys.* **16**, 013056 (2014).
- [33] N. A. Bogdanov, V. M. Katukuri, J. Romhányi, V. Yushankhai, V. Kataev, B. Büchner, J. van den Brink, and L. Hozoi, Orbital reconstruction in nonpolar tetravalent transition-metal oxide layers, *Nat. Commun.* **6**, 7306 (2015).
- [34] R. Yadav, M. Pereiro, N. A. Bogdanov, S. Nishimoto, A. Bergman, O. Eriksson, J. van den Brink, and L. Hozoi, Heavy-mass magnetic modes in pyrochlore iridates due to dominant Dzyaloshinskii-Moriya interaction, *Phys. Rev. Materials* **2**, 074408 (2018).
- [35] H. J. Werner, P. J. Knowles, G. Knizia, F. R. Manby, and M. Schütz, Molpro: a general-purpose quantum chemistry program package, *WIREs Comput. Mol. Sci.* **2**, 242 (2012).
- [36] See Supplemental Material at <http://link.aps.org/supplemental/10.1103/PhysRevResearch.4.033025> for the details of the quantum chemistry methods and exact diagonalization calculations. Cluster size dependence of effective Kitaev-Heisenberg parameters is also discussed.
- [37] S. Nishimoto, V. M. Katukuri, V. Yushankhai, H. Stoll, U. K. Rößler, L. Hozoi, I. Rousochatzakis, and J. van den Brink, Strongly frustrated triangular spin lattice emerging from triplet dimer formation in honeycomb Li_2IrO_3 , *Nat. Commun.* **7**, 10273 (2016).
- [38] Y. Li, S. M. Winter, and R. Valentí, Role of Hydrogen in the Spin-Orbital-Entangled Quantum Liquid Candidate $\text{H}_3\text{LiIr}_2\text{O}_6$, *Phys. Rev. Lett.* **121**, 247202 (2018).
- [39] R. Yadav, S. Rachel, L. Hozoi, J. van den Brink, and G. Jackeli, Strain- and pressure-tuned magnetic interactions in honeycomb Kitaev materials, *Phys. Rev. B* **98**, 121107(R) (2018).
- [40] V. M. Katukuri, R. Yadav, L. Hozoi, S. Nishimoto, and J. van den Brink, The vicinity of hyper-honeycomb $\beta\text{-Li}_2\text{IrO}_3$ to a three dimensional Kitaev spin liquid state, *Sci. Rep.* **6**, 29585 (2016).